Model of the boundary layer of a vacuum-arc magnetic filter

F. Minotti, L. Giuliani, D. Grondona, H. Della Torre, and H. Kelly

Citation: J. Appl. Phys. **113**, 113303 (2013); doi: 10.1063/1.4795604
View online: http://dx.doi.org/10.1063/1.4795604
View Table of Contents: http://jap.aip.org/resource/1/JAPIAU/v113/i11
Published by the American Institute of Physics.

Model of the boundary layer of a vacuum-arc magnetic filter

F. Minotti, L. Giuliani, D. Grondona, H. Della Torre, and H. Kelly
Departamento de Física, FCEyN, Universidad de Buenos Aires, Instituto de Física del Plasma, CONICET-UBA, Cdad. Universitaria, Pab.I, 1428 Buenos Aires, Argentina

(Received 29 October 2012; accepted 4 March 2013; published online 18 March 2013)

A model is developed to describe the electrostatic boundary layer in a positively biased magnetic filter in filtered arcs with low collisionality. The set of equations used includes the electron momentum equation, with an anomalous collision term due to micro-instabilities leading to Bohm diffusion, electron mass conservation, and Poisson equation. Analytical solutions are obtained, valid for the regimes of interest, leading to an explicit expression to determine the electron density current to the filter wall as a function of the potential of the filter and the ratio of electron density at the plasma to that at the filter wall. Using a set of planar and cylindrical probes it is verified experimentally that the mentioned ratio of electron densities remains reasonably constant for different magnetic field values and probe bias, which allows to obtain a closed expression for the current. Comparisons are made with the experimentally determined current collected at different sections of a positively biased straight filter. © *2013 American Institute of Physics*.
[http://dx.doi.org/10.1063/1.4795604]

INTRODUCTION

Vacuum arcs are used in many important applications, such as film deposition of different materials and ion implantation. Their good characteristics of high ion densities and high degree of ionization are somehow lessened by their tendency to generate macroparticles along with the arc plasma. A common means to reduce the macroparticle to plasma ratio is to employ a magnetic filter. In these devices, either straight or curved, the magnetic lines guide and concentrate the plasma while the macroparticles follow essentially ballistic trajectories. Appropriate design of the filter thus allows an effective reduction of the mentioned ratio in determined regions.[1–4] In general, at the practical values of the magnetic field employed (tens of mT) only the electrons are effectively tied to the magnetic lines (their magnetic gyro-radius is small compared to the filter minor dimension), the ions are confined by the electrostatic potential resulting from charge separation. Moreover, the plasma diffusive loses into the filter walls can be reduced, between certain limits, by positively biasing the filter.[5] In the boundary layer between the plasma and the filter wall the electrons diffuse to the wall across the magnetic field, and the ions are repelled from the wall by the electric field. The determination of the structure of this boundary layer, for a given set of plasma and filter parameters, is essential to account for the plasma losses and filter efficiency, as well as to determine appropriate boundary conditions for the plasma in fluid-like numerical simulations.

Models so far employed rely on electron-ion collisions[6,7] and are thus applicable to relatively high density plasmas, typically with number densities above $10^{20}\,m^{-3}$, characteristic of high current (kA) arcs. The model presented here is applicable to low to medium current arcs (about hundred Ampère) with plasma densities of order $10^{17}\,m^{-3}$, for which Coulomb collisions are in general negligible, in the sense that the collisional mean-free path of electrons is comparable to the filter dimensions. The difficulty in this non-collisional regime is that a mechanism for diffusion across the magnetic field is needed to explain the losses observed in the experiments. It was argued in a previous work that anomalous collisions due to micro-instabilities lead to a Bohm-like diffusion, together with an anomalous ion friction term, which can explain the observed dynamics of a non-collisional plasma in a straight magnetic filter.[8] It was argued there that these anomalous effects are mediated by rapid, small scale electric fluctuations, triggered by plasma micro-instabilities, as electron drift or lower-hybrid unstable modes, as extensively studied theoretically and experimentally for magnetron[9,10] and other discharges.[11] In particular, it was found that the model which correctly reproduced the experiment indicated larger fluctuating energies for ions than for electrons, characteristic of the instability of lower hybrid modes reaching its saturation by absorption of the wave energy by the ions, which is possible in the cases of cross-field density gradients and cross-field relative motion of both species,[12] conditions that are expected to hold in the plasma close to the biased filter wall.

In the following sections we develop a model along these lines for the current collected by a positively biased probe with surface parallel to the magnetic field. The model is completed by experimentally verifying that the electron density at the probe surface, relative to that of the plasma, has very little dependence on to the probe bias and magnetic field value, thus allowing to obtain a closed expression for the probe characteristic.

MODEL

To model the boundary layer we consider the electron fluid equation, neglecting the inertial term, in the stationary regime for the geometry depicted in Fig. 1, with the magnetic field B along the y direction

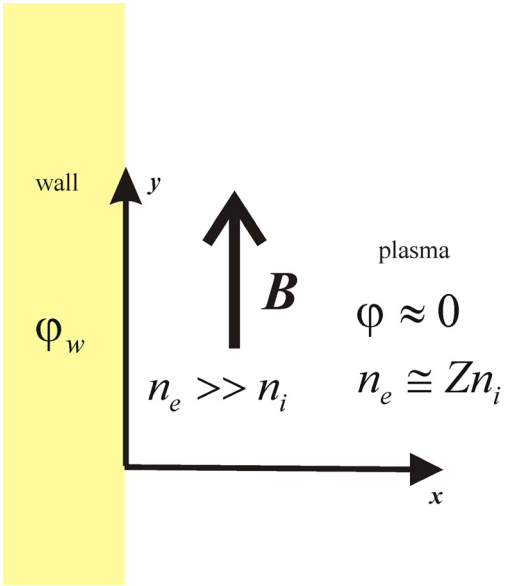

FIG. 1. Coordinate axes used for the boundary layer model. Also indicated are some of the relevant parameters and plasma conditions assumed in the model.

$$-\frac{1}{n_e}\frac{dp_e}{dx} - e(E_x - u_z B) - m_e \nu_{eff} u_x = 0,$$
$$-e\,u_x B - m_e \nu_{eff} u_z = 0,$$

where e is the absolute value of the electron charge, m_e the electron mass, n_e the electron number density, $p_e = n_e T_e$ is the electron pressure (with the electron temperature T_e in energy units), $\mathbf{u}$ the electron fluid velocity, ν_{eff} the effective collision frequency, and $\mathbf{E} = -\nabla\varphi$ the electric field. Assuming a constant T_e one obtains from these equations the electron fluid velocity normal to the wall

$$u_x = -\frac{T_e}{m_e \nu_{eff}(1 + \omega_{ce}^2/\nu_{eff}^2)}\frac{d\ln n_e}{dx} + \frac{e}{m_e \nu_{eff}(1 + \omega_{ce}^2/\nu_{eff}^2)}\frac{d\varphi}{dx}, \quad (1)$$

where $\omega_{ce} = eB/m_e$ is the electron cyclotron frequency.

The ions are considered in mechanical equilibrium in the x direction so that

$$Ze\varphi + T_i \ln n_i = T_i \ln n_{ip}, \quad (2)$$

where Z is the ion charge state, T_i is the ion temperature, n_i the ion number density, and n_{ip} that corresponding to the plasma, for which the reference for the electrostatic potential, $\varphi = 0$, is taken.

The system of equations is completed with the continuity equation for the electrons

$$\frac{d}{dx}(n_e u_x) = 0, \quad (3)$$

and Poisson equation (ε_0 is the vacuum permittivity)

$$\frac{d^2\varphi}{dx^2} = \frac{e}{\varepsilon_0}(n_e - Zn_i). \quad (4)$$

As mentioned before, in the kind of vacuum arcs we consider, with ion number densities of order $10^{17}\mathrm{m}^{-3}$, the classical collision frequency is too low to explain the observed plasma losses to the filter. We thus consider that an enhanced collision frequency takes place, which corresponds to $\nu_{eff} = \alpha\omega_{ce}$, with $\alpha = \tilde{\alpha}/2 - \sqrt{(\tilde{\alpha}/2)^2 - 1}$ and $\tilde{\alpha} \cong 6 - 25$.[8,13]

Equation (3) can be expressed as

$$n_e u_x = -j_e/e = const., \quad (5)$$

with j_e the electron current density (considered positive), while Eq. (2) is recast as

$$n_i = n_{ip}\exp(-Ze\varphi/T_i). \quad (6)$$

If we additionally define the non-dimensional potential

$$\phi \equiv e\varphi/T_e$$

and the non-dimensional auxiliary function

$$G(\xi) \equiv \frac{n_e}{Zn_{ip}}\exp(-\phi) = \frac{n_e}{n_{ep}}\exp(-\phi),$$

where $n_{ep} = Zn_{ip}$ is the electron density in the plasma, the full set of Eqs. (1)–(4) reduces to

$$\frac{dG}{d\xi} = K\exp(-\phi), \quad (7)$$

$$\frac{d^2\phi}{d\xi^2} = G(\phi)\exp(\phi) - \exp(-\tau\phi), \quad (8)$$

where $\xi \equiv x/\lambda$, with λ the Debye length $\lambda = \sqrt{\varepsilon_0 T_e/(e^2 n_{ep})}$, with also

$$\tau \equiv ZT_e/T_i \quad (9)$$

and

$$K = \tilde{\alpha} j_e B/(j_0 B_0), \quad (10)$$

where the constants j_0 and B_0, with units of electric current density and magnetic field, respectively, are given by

$$j_0 = en_{ep}\sqrt{T_e/m_e}, \quad (11)$$

$$B_0 = \sqrt{n_{ep} m_e/\varepsilon_0}. \quad (12)$$

The use of the electron mass m_e in these expressions is only a notational convenience, as it cancels out in relation (10).

The boundary conditions satisfied by the system (7) and (8) are $\phi(\xi = 0) = \phi_w$ (ϕ_w being the nondimensional potential of the filter wall relative to the plasma), together with $\phi = 0$ and $G = 1$ in the quasi-neutral plasma, $\xi \to \infty$.

Using the notation $\phi' \equiv d\phi/d\xi$ the system (7) and (8) can be expressed as

$$\phi'\frac{dG}{d\phi} = K\exp(-\phi), \quad (13)$$

$$\phi' \frac{d\phi'}{d\phi} = G(\phi)\exp(\phi) - \exp(-\tau\phi). \tag{14}$$

We now solve approximately the system (13) and (14) starting by assuming (and afterward verifying) that for large enough values of ϕ one can write

$$\phi' = -A\phi^{\gamma}, \tag{15}$$

for some constants A and γ, which allows to solve Eq. (13) to yield

$$G(\phi) = \frac{K}{A}\Gamma_{1-\gamma}(\phi), \tag{16}$$

with $\Gamma_{1-\gamma}$ the incomplete Gamma function of order $1-\gamma$. No integration constant appears in Eq. (16) because $G(\phi)\exp(\phi)$ is the (non-dimensional) electron density, which must decrease as ϕ increases, due to constancy of the electron current density (Eq. (5)). A non zero integration constant would contribute an exponential growth of the electron density with ϕ.

Use of Eqs. (15) and (16) in Eq. (14) leads to

$$\gamma A^3 \phi^{2\gamma-1} = K\Gamma_{1-\gamma}(\phi)\exp(\phi) - \exp(-\tau\phi). \tag{17}$$

As $\Gamma_{1-\gamma}(\phi)\exp(\phi) \to \phi^{-\gamma}$ for large values of ϕ, and as for usual plasma conditions τ is amply larger than one, Eq. (17) is satisfied for large enough values of ϕ when $\gamma = 1/3$ and $A = (3K)^{1/3}$, yielding

$$\phi' = -(3K\phi)^{1/3}, \tag{18}$$

$$G(\phi) = K^{2/3}(3\phi)^{-1/3}\exp(-\phi). \tag{19}$$

With expressions (18) and (19) the approximations made can be quantified, resulting in relative errors below 10% when $\phi > 2$.

The final goal is to express the current density to the wall, given the potential of the wall relative to the plasma, ϕ_w. In order to do this one must determine the value of K for given ϕ_w and use relation (10) to obtain j_e. Without any further assumption it is not possible to determine K given ϕ_w. Usually, in order to close the problem, either the extension of the boundary layer, ξ_p,[7] or the ratio of the electron density at the wall, n_{ew}, to that of the plasma, n_{ep},[6] is assumed fixed.

According to Eq. (19) we have

$$\frac{n_{ew}}{n_{ep}} = G(\phi_w)\exp(\phi_w) = K^{2/3}(3\phi_w)^{-1/3}, \tag{20}$$

so that using Eq. (10) with the K determined by Eq. (20), the current density to the wall is

$$j_e = j_0 \frac{B_0(3\phi_w)^{1/2}}{\tilde{\alpha}B(n_{ep}/n_{ew})^{3/2}}. \tag{21}$$

On the other hand, an estimation of the boundary layer thickness can be obtained by integrating Eq. (18) between $\xi = 0$ (where $\phi = \phi_w$) and $\xi = \xi_p$ (where $\phi \cong 0$) to obtain

$$\xi_p = \frac{(3\phi_w)^{2/3}}{2K^{1/3}}. \tag{22}$$

The resulting expression of K replaced in Eq. (10) gives

$$j_e = j_0 \frac{9B_0\phi_w^2}{8\tilde{\alpha}B\xi_p^3}. \tag{23}$$

It is thus seen from expressions (21) and (23) that assuming either fixed n_{ew}/n_{ep} or fixed ξ_p leads to different functional relations between j_e and ϕ_w, which can in principle be checked experimentally, as is done in the next sections.

EXPERIMENTAL SETUP

In order to check which of the two relations (21) and (23) fits better the experimentally determined current densities, we employ the experimental setup represented in Fig. 2. The vacuum chamber is a stainless steel cylinder 25 cm long with a 10 cm (inner) diameter. The chamber pressure was maintained at a base pressure $<10^{-2}$ Pa during the whole arc discharge with an oil diffusion pump. A grounded copper cathode (5 cm in length and 1 cm in diameter) is located in front of an annular anode with an aperture of 5 cm and a thickness of 2 cm. The distance between the cathode frontal surface and the closest plane of the anode is 1 cm. The lateral surface of the cathode was covered with a Pyrex insulator, physically separated from the cathode, in order to ensure that the ion emission was through the cathode front surface. The entrance of the magnetic filter was placed at the end of the anode, separated by a 1 cm insulating ring, at 4 cm from the cathode frontal surface. The magnetic field is generated by an external coil wrapped around a stainless steel tube (22 cm long, 5 cm inner diameter). The coil (3 layers of 30 turns each) was fed with dc current from an independent power source. The magnetic field strength was measured with a calibrated Hall probe, and the magnetic field intensity was characterized with the value measured at the duct center $B_{\max}$. The arc was pulsed for about 35 ms, with an arc peak current of (450 ± 20) A and an interelectrode voltage of (45 ± 5) V. More details can be found in Ref. 14.

In order to determine the ion number density, electron temperature, and plasma potential relative to ground, probe measurements were performed at 16 cm from the cathode along the filter axis for $B_{\max} = 20$, 29, and 43 mT. A plane disc probe of 6 mm diameter was connected to a dc source

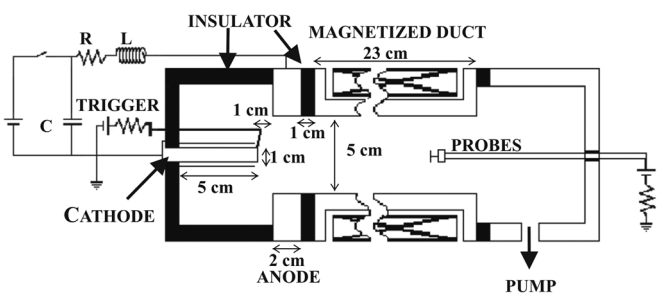

FIG. 2. Sketch of the experimental setup. Indicated is the planar probe used to determine the plasma parameters. At the same position the cylindrical probe is used for the validation of the model.

and grounded through a 10 Ω resistance to measure the probe current (I_s) as a function of the probe potential (V_s). The electrical signals were registered using a four-channel digitizing oscilloscope Tektronix TPS 2014 (100 MHz, 1 GS/s). The surface of the probe was perpendicular to the duct axis so as to use the standard Langmuir-Lam[15] theory to determine densities and temperatures from the measurements. The Lam expression for the probe current includes the effect of the drifting energetic ions, and although it was derived for spherical or cylindrical probes, in the limit considered of large ion drift energies, compared to the electron temperature, only the cross-sectional area of the probe contributes, and so it can be used for the planar case.

To measure the current reaching a surface parallel to the magnetic field lines, the plane probe was replaced by a cylindrical collector of 1.5 mm in diameter and 15 mm long, with its axis along the duct axis. A characteristic I_s-V_s curve was obtained using the same electric circuit as the one used with the planar probe for the same B_{max} values of 20, 29, and 43 mT.

RESULTS

From the I_s-V_s curve corresponding to the planar probe for $B_{max} = 29$ mT, using Langmuir-Lam theory for copper ions of kinetic energy 57 eV, and charge number $Z = 2$, an electron temperature of $T_e = 4.7 \pm 0.1$ eV, an ion number density $n_{ip} = (1.0 \pm 0.3) \times 10^{17}\,m^{-3}$, and a plasma potential relative to ground of (43 ± 3) V were obtained for this magnetic field value at the probe position. In the same manner it was verified that at this position the electron temperature and plasma potential do not vary with the magnetic field value, while the ion density at the same location resulted in $n_{ip} = (4.9 \pm 1.6) \times 10^{16}\,m^{-3}$ for $B_{max} = 20$ mT and $n_{ip} = (1.9 \pm 0.6) \times 10^{17}\,m^{-3}$ for $B_{max} = 43$ mT.

For the same set of magnetic field values the planar probe was replaced by the cylindrical probe with its axis aligned with the magnetic field. Using the measured values of ion density and electron temperature one can evaluate the fraction of the current that is collected by the small front surface of the cylindrical probe that is not parallel to the magnetic field. The calculated collected current by this front surface is smaller than the total collected current by at least one order of magnitude and can thus be neglected.

A practical problem is the alignment of the probe lateral surface with the magnetic field, as even a small misalignment results in relatively large currents collected when the probe is at the plasma potential, whereas no current is predicted in a collisionless model for a well aligned probe.[16] Measured values with the probe at the plasma potential resulted in about 20% of the free streaming value of electron current, corresponding to about a 10° angle between probe surface and magnetic field. It was not possible to maintain perfect alignment of the relatively long probe during the set of discharges used to determine averaged values of the measured currents for each magnetic field value, and so in order to compare with the theory, the current collected when the probe is biased at the plasma potential, previously determined from the planar probe measurements, was substracted from the values corresponding to higher potentials.

Fig. 3 shows the currents collected by the cylindrical probe for the three values of the magnetic field as a function of its non-dimensional potential, ϕ_w, relative to the plasma, for positive bias relative to the plasma, up to approximately 50 V. In this log-log scale it can be observed that for the three values of the magnetic field the behavior is rather well approximated by a power law function and that the square root dependence predicted by Eq. (21) is rather good and much better than the power 2 predicted by Eq. (23) for constant layer width. For a better visualization, Fig. 4 shows, as a function of $\phi_w^{1/2}$, the values of

$$\frac{j_e B}{3^{1/2} j_0 B_0}. \tag{24}$$

According to Eq. (21) the slopes in this plot correspond to the inverse of $\tilde{\alpha}(n_{ep}/n_{ew})^{3/2}$. The linear fit for all field values is also shown in the figure, allowing to determine the value

$$\frac{1}{\tilde{\alpha}(n_{ep}/n_{ew})^{3/2}} = (3 \pm 2) \times 10^{-3}. \tag{25}$$

With the value (25), expression (21) can be written in terms of fully dimensional quantities as

$$j_e = (5 \pm 3) \times 10^{-3} \frac{(e n_{ep})^{3/2}}{B} \left(\frac{\varphi_w}{\varepsilon_0}\right)^{1/2}, \tag{26}$$

where φ_w is the (positive) potential of the wall relative to the quasi-neutral plasma in its proximity.

MODEL APPLICATION AND DISCUSSION

Relation (26) was used to model the current collected by the magnetic filter in the same apparatus used before. The filter was biased at a nominal potential (open circuit) of about 80 V relative to the grounded cathode, and for each of four different values of the magnetic field the current collected by

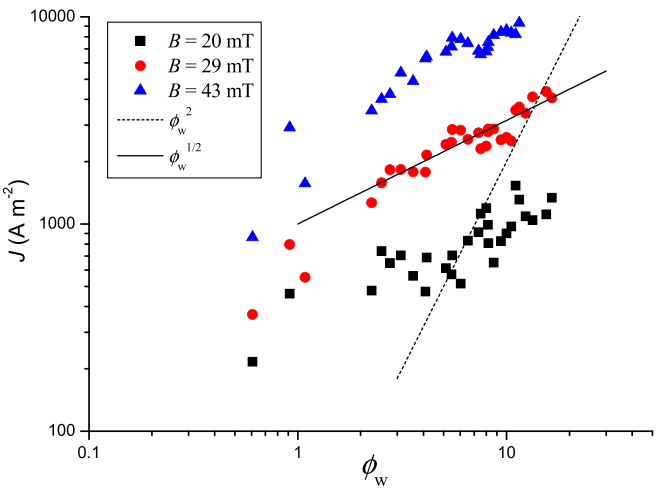

FIG. 3. Log-log plot of the current density collected by the cylindrical probe, for three different values of the magnetic field, as a function of the non-dimensional potential ϕ_w of the probe relative to that of the plasma. Also included are the two lines indicating power law behavior with exponents 1/2 and 2.

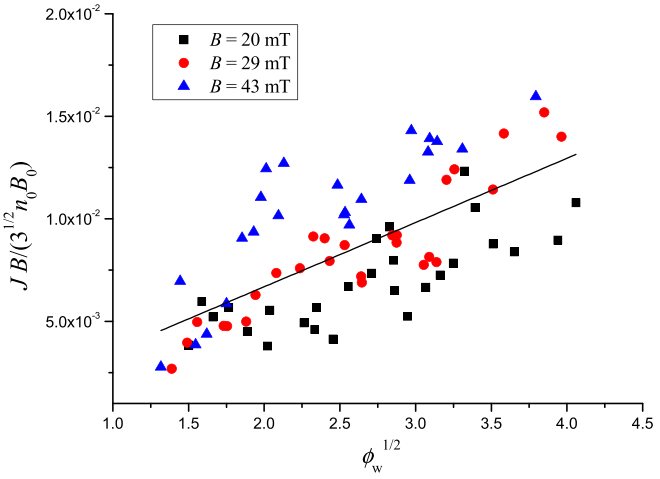

FIG. 4. Non-dimensional product of current density collected by the cylindrical probe times the magnetic field value, for three different values of the magnetic field, as a function of the square root of the non-dimensional potential ϕ_w of the probe relative to that of the plasma. Also included is the line showing the best linear fit.

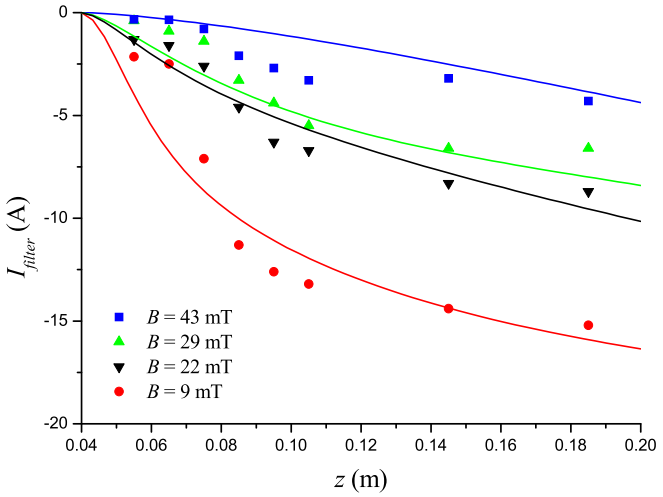

FIG. 5. Current collected by sections of the filter up to the distance z from the cathode, for four different maximum values of the magnetic field. The symbols indicate the experimental values and the lines the theoretical results.

the filter was measured through the voltage drop on a small value resistance ($\sim 1\,\Omega$) in series with the biasing circuit. A large metallic disk, of the same radius as the filter, was used in order to prevent the filter from collecting current beyond the disk axial position. In this way, the current collected by increasingly larger sections of the filter was measured and compared with the predictions of the model (26). The model employed for the plasma was the same as in Ref. 8, which allows to determine, among other parameters, the values of density and electrostatic potential for the plasma as functions of axial and radial position.

The four values of the (maximum) magnetic field used in the experiment were 9.2, 22.4, 29.3, and 43 mT. For each of these values the model was run to obtain the plasma density and plasma potential at the filter wall, and Eq. (26) was used to match the experimentally determined current as a function of the axial position, with the filter potential as only parameter in each case, also taking a single value inside the error band of the nondimensional coefficient in Eq. (26), which resulted for the best fit to be 3×10^{-3}.

As the filter collects relatively large currents its potential decreases, relative to the nominal 80 V, due to the internal resistance of the power source and the resistance used to measure the current. In Fig. 5 the experimental values of current collected at different axial positions are shown in symbols for each value of the magnetic field. In the same figure the values given by Eq. (26) are shown in full lines. The filter potentials (relative to the grounded cathode) that fitted the results were 44, 53, 57, and 76 V for the magnetic field values 9.2, 22.4, 29.3, and 43 mT, respectively. This is consistent with an internal power-source resistance of a little over $1\,\Omega$ in series with the $1\,\Omega$ measuring resistance. It is interesting to mention that the difference of potential between the filter and the plasma close to the filter (in the region far from the filter entry, where the plasma potential is uniform) resulted in all cases only of a few volts.

Also worth mentioning is that the measured value of $\tilde{\alpha}(n_{ep}/n_{ew})^{3/2}$, Eq. (25), corresponds to $n_{ep}/n_{ew} \cong 8$ for the classical Bohm value $\tilde{\alpha} = 16$, while for the accepted values of $\tilde{\alpha}$, the ratio n_{ep}/n_{ew} ranges between 6 and 14, very similar magnitudes to the value 10 used in Ref. 6 for the collisional case.

CONCLUSIONS

A model was presented for the collisonless boundary layer at the wall of a positively biased magnetic filter, which by construction has a magnetic field parallel to the wall. For the plasma densities in the experiments considered in this work the mean free path for Coulomb collisions is of the order of the filter dimensions,[8] and so the mechanisms for electron diffusion across the magnetic lines towards the filter wall was thought as associated to micro-instabilities, leading to a Bohm-like anomalous diffusion. As with most boundary layer models, an assumption is needed to obtain closed results like, for instance, the current-voltage characteristic. The assumption experimentally favored was that the ratio of electron density in the plasma, relative to that at the wall, can be considered approximately independent of the values of magnetic field and filter bias, leading to a collected current density that grows as the square root of the filter potential relative to the plasma, with a coefficient proportional to the inverse of the magnetic field value (Eq. (26)). An important practical point is that the large currents to the filter wall resulting from the anomalous diffusion, limit the filter bias to a few volts above the plasma potential in the non-collisional regime considered, very much like an anode layer in a non-magnetized plasma.

Finally, although a magnetic filter was considered, the result (26) should be applicable to the metallic walls of other magnetic systems in the conditions studied: low collisionality, magnetic field parallel to the wall, and positive bias.

[1]J. Storer, J. E. Galvin, and I. G. Brown, "Transport of vacuum arc plasma through straight and curved magnetic ducts," J. Appl. Phys. **66**(11), 5245–5250 (1989).
[2]S. Anders, A. Anders, K. M. Yu, X. Y. Yao, and I. G. Brown, "On the macroparticle flux from vacuum arc cathode spots," IEEE Trans. Plasma Sci. **21**, 440–446 (1993).

[3]H. Kelly, L. Giuliani, and F. Rausch, "Characterization of the ion emission in a pulsed vacuum arc with an axial magnetic field," J. Phys. D: Appl. Phys. **36**, 1980–1986 (2003).
[4]A. Anders, *Cathodic Arcs: From Fractal Spots to Energetic Condensation* (Springer, New York, 2008), Chap. 7.
[5]A. Anders, S. Anders, and I. G. Brown, "Effect of duct bias on transport of vacuum arc plasmas through curved magnetic filters," J. Appl. Phys. **75**, 4900–4905 (1994).
[6]M. Keidar and I. I. Beilis, "Plasma-wall sheath in a positive biased duct of the vacuum arc magnetic macroparticle filter," Appl. Phys. Lett. **73**, 306–308 (1998).
[7]S. T. Zhang, Y. C. Zhang, P. K. Chu, and I. G. Brown, "Wall sheath and optimal bias in magnetic filters for vacuum arc plasma sources," Appl. Phys. Lett. **80**, 365–367 (2002).
[8]F. Minotti, L. Giuliani, D. Grondona, H. D. Torre, and H. Kelly, "Model with anomalous diffusion and friction for a vacuum-arc plasma jet in a straight magnetic filter," IEEE Trans. Plasma Sci. **39**, 2014–2021 (2011).
[9]E. Martines, M. Zuin, V. Antoni, R. Cavazzana, G. Seriani, M. Spolaore, and C. Nakashima, "Experimental investigation of low-frequency waves propagating in a direct current planar magnetron plasma," Phys. Plasmas **11**, 1938–1946 (2004).
[10]E. Bultinck, S. Mahieu, D. Depla, and A. Bogaerts, "The origin of Bohm diffusion, investigated by a comparison of different modeling methods," J. Phys. D: Appl. Phys. **43**, 292001 (2010).
[11]T. Hurtig, N. Brenning, and M. A. Raadu, "The role of high frequency oscillations in the penetration of plasma clouds across magnetic boundaries," Phys. Plasmas **12**, 012308 (2005).
[12]S. Krishan and M. P. Ravindra, "Ion heating by the lower hybrid mode," Phys. Rev. Lett. **34**, 938–940 (1975).
[13]J. W. Bradley, S. Thompson, and Y. A. Gonzalvo, "Measurement of the plasma potential in a magnetron discharge and the prediction of the electron drift speeds," Plasma Sources Sci. Technol. **10**(3), 490–501, 507 (2001).
[14]L. Giuliani, D. Grondona, H. Kelly, and F. O. Minotti, "On the plasma rotation in a straight magnetized filter of a pulsed vacuum arc," J. Phys. D: Appl. Phys. **40**, 401–408 (2007).
[15]S. H. Lam, "Unified theory of the Langmuir probe in a collisionless plasma," Phys. Fluids **8**, 73–83 (1965).
[16]U. Daybelge and B. Bein, "Electric sheath between a metal surface and a magnetized plasma," Phys. Fluids **24**, 1190–1194 (1981).